Modulation coding for pixel-matched holographic data storage

Geoffrey W. Burr, Jonathan Ashley, Hans Coufal, Robert K. Grygier, John A. Hoffnagle, C. Michael Jefferson, and Brian Marcus

Holographic Optical Storage Team, IBM Almaden Research Center, 650 Harry Road, San Jose, California 95120

Received October 24, 1996

We describe a digital holographic storage system for the study of noise sources and the evaluation of modulation and error-correction codes. A precision zoom lens and Fourier transform optics provide pixel-to-pixel matching between any input spatial light modulator and output CCD array over magnifications from 0.8 to 3. Holograms are angle multiplexed in $LiNbO_3$:Fe by use of the 90° geometry, and reconstructions are detected with a 60-frame/s CCD camera. Modulation codes developed on this platform permit image transmission down to signal levels of ~2000 photons per ON camera pixel, at raw bit-error rates (BER's) of better than 10^{-5}. Using an 8–12–pixel modulation code, we have stored and retrieved 1200 holograms (each with 45,600 user bits) without error, for a raw BER of $<2 \times 10^{-8}$. © 1997 Optical Society of America

Volume holography is currently the subject of widespread interest as a fast-readout-rate, high-capacity digital data-storage technology.[1–3] These desirable features come from the superposition of multiple data pages, each containing as many as a million pixels accessed in parallel at one page per millisecond. Researchers recently demonstrated the storage of 10,000 superimposed holograms,[1] the use of digital-processing techniques for data extraction,[3] nonmechanical data access,[2] and high areal density (10 bits/μm^2) in thin materials.[4] These experiments demonstrated the potential for either high capacity or fast readout but not both, because no experiments have implemented a practical optical–electronic conversion of the massively parallel data pages that are needed to attain these goals simultaneously.

In part, this is due to the difficulty of imaging the input pixel grid of a spatial light modulator (SLM) onto an output grid of CCD pixels. Mismatch between the pixel spacings of the SLM and the CCD is common, requiring precise nonunity magnification in the imaging optics. One proposed solution is to intersperse alignment targets with the input data, oversample at the detector, and then use postprocessing to assign small blocks of camera pixels to the appropriate input pixels.[3] However, at the desired readout rate, the complexity and cost of the electronics that one needs to perform these operations makes this approach untenable.

Another approach is to use precision optics with the goal of pixel-to-pixel matching between the input SLM and the output CCD camera. Here, each parallel data channel consists of one SLM pixel imaged onto one CCD pixel, simplifying the optical–electronic conversion tremendously. From an eventual commercial perspective, custom optics can be replicated in quantity by use of injection molding. From a research perspective, excellent pixel matching provides an extremely low bit-error-rate (BER) system, in which the effects of noise sources are easily studied. Recently, we used this approach to construct a pixel-matched tester for evaluating and comparing prospective holographic-storage materials, with a chrome-on-glass mask as the input SLM.[5] In this Letter we present what is to our knowledge the first demonstration of pixel-to-pixel matching between a real-time SLM and a video-rate CCD camera in our DEMON system. We introduce several balanced-block modulation codes and compare them in terms of the maximum user capacity within a stack of superimposed holograms.

In general, the capacity of a holographic-storage system involves a trade-off among the number of holograms, the number of pixels, and the readout rate. Any increase in the number of holograms, M, reduces diffraction efficiency η, since $\eta = [(M/\#)/M]^2$, where $M/\#$ is a constant for a given material and storage geometry.[6,7] For a given diffraction efficiency and readout beam power, P_{ref}, an increase in the number of SLM pixels per hologram, N_p, reduces the signal power available at each CCD pixel. The tradeoff between capacity and readout rate arises from the need to collect a sufficient number of photons at each pixel during the integration time t_{int}. These influences can be described by a single formula for Φ, the target number of photons per pixel for a given BER:

$$\Phi(\mathrm{BER}) = \frac{(M/\#)^2}{h\nu}\,\frac{P_{\mathrm{ref}}\,t_{\mathrm{int}}}{N_p M^2}, \tag{1}$$

where $h\nu$ is the energy per photon. As expected, any given target Φ is easier to reach with a larger $M/\#$ or more readout power P_{ref}.

Equation (1) demonstrates that a decrease in Φ can be used to improve to improve either capacity ($N_p M^2$) or readout rate ($\propto 1/t_{\mathrm{int}}$) at constant BER. Several factors, including improvements in camera efficiency, camera noise, and overall system noise, can reduce the required number of photons per pixel. Using the DEMON system, we show that the use of modulation codes can also reduce Φ.

Modulation codes transmit n bits of information with m pixels, where $m > n$. User capacity is reduced by n/m, the modulation code rate, in return for simplified signal decoding and improved BER performance. The modulation codes that we describe here are balanced- (or nearly balanced-) block codes, where each code block contains $m/2$ ON pixels and $m/2$ OFF pixels. This constraint removes the need to select an explicit threshold. Instead, the brightest $m/2$ CCD pixels are decoded as ON and the rest as OFF, and the resulting m-pixel pattern is mapped to a unique n-bit pattern

0146-9592/97/090639-03$10.00/0

label.[8] A more accurate method is to find the code word that correlates best with the received block of intensities; this can be efficiently implemented with Viterbi detection.[9] Several balanced-block codes are summarized in Table 1 in terms of minimum Hamming distance $d_{\min}$ and path memory. To cause incorrect decoding when $d_{\min} = 2$, the signal from an OFF pixel must exceed the signal from one of the ON pixels within the same block (a two-pixel swap). Codes with $d_{\min} = 4$ will actually correct for the most likely two-pixel swaps, failing for swaps involving at least two ON and two OFF pixels. The path memory of a code indicates the number of blocks involved in each decoding operation. For codes with path memory of 1, a simple correlation decoding scheme can decode each block independently (the 6:8 code requires only 13 add operations and 13 compares). With a larger path memory, the code has several states, and neighboring blocks are involved in the decoding of each block.

To compare these modulation codes in terms of the number of photons per pixel, we performed simple imaging experiments on the DEMON platform. These experiments also set a baseline performance for stored holograms of comparable signal strength. Discrepancies between imaging and hologram BER's can be studied and traced to the holographic-storage process, degradation of the imaging path during recording, or loss of fidelity during the erasure inherent in a photorefractive-recording schedule.

A schematic of the DEMON platform is shown in Fig. 1. All the optics except the argon laser are mounted upon a 45.7 cm × 161 cm plate. The 514.5-nm laser output is routed to the system via a fiber and split into object and reference paths. The object beam is expanded to overfill the input aperture of the SLM, sacrificing power for beam uniformity. Currently, we use an Epson 640 × 480 transmissive liquid-crystal panel with 42-μm pixel spacing and 41% area-fill factor. The spatially modulated beam is demagnified by a custom five-element zoom lens, forming a pixel-matched image in the zoom-lens output plane. This plane coincides with the input plane of a folded 4-F system, with two Fourier-transform lenses of 89-mm focal length. The CCD camera is a Pulnix TM6701AN with a 640 × 480 Kodak KAI-0310M CCD chip running at 60 frames/s. The CCD pixels are on a 9-μm grid. Since the zoom lens was not designed for magnifications greater than 3.0, the 42-μm spacing of the current SLM is demagnified to an 18-μm grid, and only the center 320 × 240 pixels of the SLM are seen by the camera. Since each incoming SLM image is centered on a single CCD pixel, there is no oversampling or postprocessing. The Pulnix camera is used as if it were a 320 × 240 pixel camera with 18-μm spacing and 15% area-fill factor. The camera and the SLM each have two New Focus picomotor stages for registration of the pixel grids. These permit alignment of either the SLM to the CCD or the CCD to a stored hologram and are needed only periodically, depending on changes in ambient temperature. An acousto-optic modulator, reduces the incident flux during object beam alignment.

We typically position the Fourier-transform plane 2–3 cm behind the square exit face of the 8 mm × 15 mm × 15 mm $LiNbO_3$ (0.02% Fe) crystal and use an aperture to pass only the central nine orders of the Fourier spectrum (0.81 cm^2). With this large aperture, the point-spread function is narrow, and interpixel cross talk is negligible. A Cambridge Instruments 602HC-6650 galvanometric mirror positioner (1.5-ms settling time, 1.5-μrad repeatability) is used to deflect the reference beam for angle multiplexing.

For these imaging experiments, we varied the image power by pulsing the acousto-optic modulator for only a small fraction of the camera integration period. For each image power and modulation code, we transmitted 15–180 different encoded pages, demodulated the resulting camera signal values, and compared the output data with the original input data. The measured raw BER is shown in Fig. 2 as a function of the number of photons per ON pixel. Note that there is a separation between the codes with $d_{\min} = 2$ (6:8, 8:10) and those with $d_{\min} = 4$ (4:8, 8:12). The BER for global thresholding is shown as well, and *a priori* knowledge was used to optimize the threshold of each page. Note that any practical thresholding method would incur additional errors whenever the threshold it chose to use was nonoptimal.

The scaling on the bottom axis of Fig. 2 was derived from a calibration of the 8-bit camera signal counts to the input image power, performed with a powermeter (Newport 835) in low-intensity cw light. The noise in the detection system was measured at these signal levels with uniform illumination from an integrating sphere. In units of photons per ON pixel, the standard deviation, σ_{noise}, gradually increased from 150 to 170

Table 1. Description of Modulation Codes Demonstrated in the DEMON Platform[a]

Name (n:m)	Minimum Distance	Path Memory
6:8	2	1
8:10	2	2[b]
4:8	4	2
8:12	4	3

[a]Each code encodes n information bits in m output pixels.
[b]Not exactly balanced; maintains estimates of signal levels.

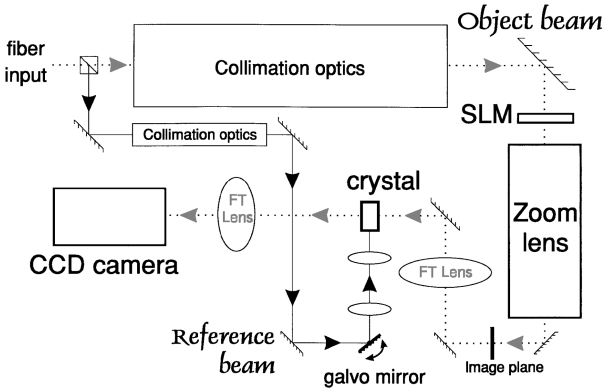

Fig. 1. Schematic of the DEMON platform. The zoom lens permits pixel-to-pixel matching between an SLM and a CCD camera. FT, Fourier transform.

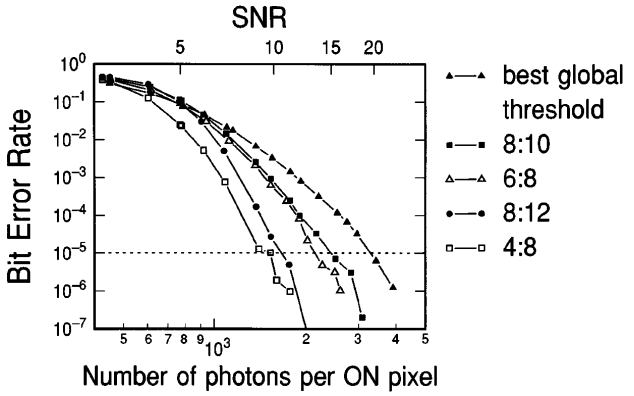

Fig. 2. Measured BER as a function of image power for several modulation codes. Camera noise was the dominant noise source. SNR, signal-to-noise ratio.

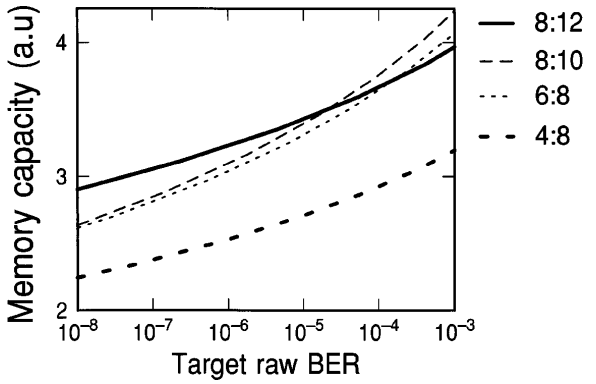

Fig. 3. Relative capacity as a function of target raw BER for several modulation codes. This quantifies the trade-off between code rate and the ability to detect weaker holograms (permitting more stored holograms).

over the wide range of signal levels shown in Fig. 2. This implies that camera noise dominated shot noise in these experiments. The signal-to-noise ratio shown at the top of Fig. 2 is the ratio of the number of signal photons to the measured σ_{noise}.

Qualitatively, Fig. 2 shows that the modulation codes return improved error performance in return for the decrease in user capacity. If these codes were to be used to increase capacity through the number of pixels per page (N_p), or to reduce the integration time (t_{int}), they would perform well: Any decrease in target Φ leads to the same factor of improvement in capacity or readout rate. However, N_p and t_{int} tend to be constrained by available components, leaving the number of holograms, M, as the free parameter to be optimized. Here the $1/M^2$ dependence of diffraction efficiency makes sacrifices in code rate less attractive. For instance, a code with a rate of 0.5 must deliver at least a fourfold decrease in Φ to double the number of holograms. At a given N_p and t_{int}, we can compare the modulation codes on the basis of the capacity within a stack of superimposed holograms, using the figure of merit $r/[\Phi(\text{BER})]^{1/2}$. Here, $r \equiv m/n$ is the modulation code rate and $\Phi(\text{BER})$ is the target number of photons per pixel at a given raw BER (from Fig. 2). In Fig. 3 we plot this capacity figure of merit as a function of the target raw BER for each modulation code.

For an error-correlation code to guarantee a user BER $< 10^{-12}$, the raw BER should be $\sim 10^{-5}$ or better (we do not consider trade-offs between the error-correction code rate and its performance). With this criterion, the three modulation codes other than the 4:8 appear to provide similar user capacity. However, the experiments presented here do not include all the noise sources expected in stored holograms. With this in mind, it might be prudent to require $<10^{-7}$ raw BER from the imaging performance, in which case the 8:12 code is the best blend of code rate and error performance.

Using the 8:12 code, we have stored and retrieved 1200 superimposed holograms in the DEMON platform. The average recording time was 0.5, and the average diffraction efficiency was 7.5×10^{-8}. There were no errors among the 55×10^6 bits reassembled from the retrieved and decoded pages. The ability of the 8:12 code to ignore simple two-pixel swaps makes this level of performance possible—the raw BER using the optimal global threshold on each page would have been approximately 4×10^{-4}. Each hologram was reconstructed with a 16.7-ms camera integration with the 8:12 decoding performed off line.

In conclusion, we have developed several balanced-block modulation codes that simplify the decoding process, permit operation at extremely low signal levels, and even provide some built-in error correction. In addition, we have demonstrated what is believed to be the first holographic-storage system with pixel-to-pixel matching between a real-time SLM and a video-rate CCD camera. We have shown that, to maintain the same capacity, the quadratic relation between diffraction efficiency and the number of holograms (the $1/M^2$ relation) requires that sacrifices in code rate be accompanied by significant performance gains. Finally, we have stored and retrieved 1200 superimposed holograms with a raw BER of $<2 \times 10^{-8}$.

This work was supported in part by the U.S. Defense Advanced Research Projects Agency under agreement MDA972-95-3-0004. We thank the members of the Holographic Data Storage Systems Consortium for helpful discussions.

References

1. D. Psaltis and F. Mok, Sci. Am. **273,** 70 (1995).
2. J. H. Hong, I. McMichael, T. Y. Chang, W. Christian, and E. G. Paek, Opt. Eng. **34,** 2193 (1995).
3. J. F. Heanue, M. C. Bashaw, and L. Hesselink, Science **265,** 749 (1994).
4. A. Pu and D. Psaltis, Appl. Opt. **35,** 2389 (1996).
5. M.-P. Bernal, H. Coufal, R. K. Grygier, J. A. Hoffnagle, C. M. Jefferson, R. M. Macfarlane, R. M. Shelby, G. T. Sincerbox, P. Wimmer, and G. Wittmann, Appl. Opt. **35,** 2360 (1996).
6. D. Psaltis, D. Brady, and K. Wagner, Appl. Opt. **27,** 1752 (1988).
7. F. H. Mok, G. W. Burr, and D. Psaltis, Opt. Lett. **21,** 896 (1996).
8. J. Heanue, M. C. Bashaw, and L. Hesselink, J. Opt. Soc. Am. A **12,** 2432 (1996).
9. J. F. Pieper, J. G. Proakis, R. R. Reed, and J. K. Wolf, IEEE Trans. Inf. Theory **4,** 458 (1978).